DOI: 10.1002/cmdc.201000348

Double Click Reaction for the Acquisition of a Highly Potent and Selective mPTPB Inhibitor

Rongjun He,[a] Zhihong Yu,[a] Yantao He,[a] Li-Fan Zeng,[a] Jie Xu,[a] Li Wu,[a, b] Andrea M. Gunawan,[b] Lina Wang,[a] Zhong-Xing Jiang,[a] and Zhong-Yin Zhang*[a, b]

Tuberculosis (TB), which is caused by *Mycobacterium tuberculosis* (Mtb), is a major worldwide threat to public health. *Mycobacterium* protein tyrosine phosphatase B (mPTPB) is a virulent phosphatase secreted by Mtb, which is essential for the survival and persistence of the bacterium in the host. Consequently, small-molecule inhibitors of mPTPB are expected to serve as anti-TB agents with a novel mode of action. Herein, we report the discovery of highly potent and selective mPTPB inhibitors using a novel, double Click chemistry strategy. The most potent mPTPB inhibitor from this approach possesses a K_i value of 160 nM and a >25-fold selectivity for mPTPB over 19 other protein tyrosine phosphatases (PTBs). Molecular docking study of the enzyme–inhibitor complex provides a rationale for the high potency and selectivity of the lead compound and reveals an unusual binding mode, which may guide further optimization effort.

Introduction

A vast array of biological phenomena, such as cell proliferation and differentiation, motility, metabolism, apoptosis, and immune responses, are regulated by protein tyrosine phosphorylation, a process that is controlled by the balanced action of protein tyrosine phosphatases (PTPs) and protein tyrosine kinases (PTKs).[1] Similar to the PTKs, unregulated PTP activity causes aberrant dephosphorylation, which is associated with many human diseases, including cancer, diabetes, and autoimmune disorders.[2] Strikingly, PTPs have also been used by pathogenic bacteria to alter host defense mechanisms for their own infectivity and/or survival in the host. For instance, *Mycobacterium* protein tyrosine phosphatase B (mPTPB) is a virulence factor from *Mycobacterium tuberculosis* (Mtb), the causative agent of tuberculosis (TB). mPTPB is secreted by Mtb into the cytoplasm of macrophages, where it mediates mycobacterial survival in the host.[3] Deletion of mPTPB impairs the ability of the mutant strain to survive in interferon-γ (IFN-γ)-activated macrophages and severely reduces the bacterial load in a clinically-relevant guinea pig model.[4]

TB is a major worldwide threat to public health, with approximately 9 million new cases reported and 1.8 million deaths each year in the world.[5] No new anti-TB drugs have been developed in close to 40 years. Traditional TB treatment requires a 6–9 months administration of multiple antibiotics targeting mycobacterial biosynthetic processes involved in cell growth, including RNA transcription, protein translation, and cell wall biogenesis. The limited effectiveness of current antibiotics and lengthy treatment lead to poor patient compliance, which is responsible for high rates of treatment failure, relapse, and emergence of multidrug-resistant (MDR) and extensively resistant (XDR) TB. The prevalence of MDR-TB and XDR-TB, coupled with the acquired immune deficiency syndrome (AIDS) epidemic since AIDS patients are sometimes co-infected with TB, underscores the urgency for the development of more effective therapies against novel TB targets.[6]

Given the essential role of mPTPB for Mtb survival in the host, there is increasing interest in developing mPTPB inhibitors as novel anti-TB agents. Because mPTPB inhibitors have no structural or mechanistic overlap with current drugs used for TB treatment and function within the cytosol of host macrophage, they have great potential to target the intracellular pool and compliment/synergize with existing therapeutic strategies. Moreover, since mPTPB is secreted into the cytosol of host macrophages, drugs targeting mPTPB are not required to penetrate the waxy mycobacterial cell wall, which is a major barrier blocking translation of target inhibition to activity against the intact pathogen. Consequently, specific mPTPB inhibitors may have therapeutic value with a unique mode of action.

To date, a limited number of mPTPB inhibitors have been reported. Those described in the literature include indoles discovered by biology-oriented synthesis,[7a–c] indolizines synthesized via solid phase synthesis,[7d] isoxazoles designed through a substrate-based fragment approach,[7e] oxamic acid derivatives discovered by a homogeneous plate assay,[7f] phenylisox-

[a] Dr. R. He, Dr. Z. Yu, Dr. Y. He, Dr. L.-F. Zeng, Dr. J. Xu, L. Wu, L. Wang, Dr. Z.-X. Jiang, Prof. Dr. Z.-Y. Zhang
Department of Biochemistry and Molecular Biology
Indiana University School of Medicine
635 Barnhill Drive, Indianapolis, IN 46202 (USA)
Fax: (+1) 317-274-4686
E-mail: zyzhang@iupui.edu

[b] L. Wu, A. M. Gunawan, Prof. Dr. Z.-Y. Zhang
Chemical Genomics Core Facility
Indiana University School of Medicine
635 Barnhill Drive, Indianapolis, IN 46202 (USA)

Supporting information for this article is available on the WWW under http://dx.doi.org/10.1002/cmdc.201000348.

azole carboxylic acids,[7g] and most recently salicylic-acid-based inhibitors synthesized via Click chemistry.[7h] Unfortunately, the potency and selectivity for many of the reported compounds are still modest, which is not surprising since PTPs share a conserved active site, rendering the acquisition of highly selective PTP inhibitors an extremely challenging endeavor. Moreover, due to the complexity of the structures, these inhibitors require multistep synthesis (more than 7 steps for all reported inhibitors) with low yields, which could hinder their further development. Herein, we present our discovery of a potent and selective, yet easily accessible, mPTPB inhibitor synthesized via a novel double Click chemistry strategy.

Results and Discussion

It has been recognized that phosphotyrosine (pTyr) alone is not sufficient for high-affinity binding, and residues flanking pTyr are important for PTP substrate recognition.[8] Thus, an effective strategy for the acquisition of potent and selective PTP inhibitors is by tethering a non-hydrolyzable pTyr mimetic to an appropriately functionalized moiety in order to engage both the active site and a unique nearby subpocket.[8,9] Click chemistry refers to the 2+3 cycloaddition between an alkyne and an azide,[10] which is ideally suitable for connecting two fragments together. Because of its high yield and selectivity, excellent functional group tolerance, and robust reaction conditions, the Click reaction has been widely used in medicinal chemistry for library construction, lead optimization, and cell-based imaging.[11] Since Click reactions can be conducted in aqueous solution in the absence of deleterious reagents, libraries generated by Click reactions could be directly screened in situ for enzyme inhibitors and protein ligands. In a conventional Click reaction, an alkyne functional group is installed into a core component, which then reacts with a set of azide-containing fragments in a 1:1 mode to afford desired reaction products (Scheme 1a). We have recently employed Click chemistry for the construction of salicylic-acid-based focused libraries to target both the PTP active site and its adjacent, peripheral secondary binding sites.[7h,12,13] Although several bidentate inhibitors with excellent cellular activity were identified, the inhibitory potencies were still modest, with IC_{50} values in the low micromolar range.

As an initial attempt to further increase interactions with peripheral pockets surrounding the active site, we were interested in introducing two alkyne groups into the core structure, which would enable a core to react with an azide in a 1:2 fashion, thus creating a tridentate molecule (Scheme 1b). The additional fragment in the molecule would provide extra interactions with the enzyme, hence the potency and selectivity could be improved. Another advantage is that, since one more fragment will be incorporated into the molecule, we could choose cores that are easily accessible and structurally less complicated for library assembly (Scheme 2a), which may save a significant amount of time and effort for the synthesis of cores.

To assess the effectiveness and feasibility of the double Click reaction approach for PTP inhibitor design, we prepared five benzoic- and naphthoic-acid-based cores with two alkyne functional groups attached, as shown in Scheme 2b. The reasons we chose these cores are that they represent the simplest pTyr substrate analogues to fit into the positively charged active site of the PTPs and that they can be easily synthesized in two steps with high yields and large quantities from commercially available and inexpensive precursors. The synthesis is composed of alkylation followed by hydrolysis, which is illustrated in Scheme 2b. Subsequently, these five cores were purified by reversed-phase preparative HPLC and screened against mPTPB for inhibitory activity. We found that **L1**, **L2**, and **L4** showed no inhibition of the enzyme at 200 μM concentration, while **L3** and **L5** inhibited mPTPB with an IC_{50} value of 50 and 75 μM, respectively. As an initial proof-of-concept, we decided to focus on core **L5** for library construction using the double Click strategy. The azides used in this study were prepared from 53 amines (Scheme 2c), as described previously.[7h,13]

To prepare the library, we coupled **L5** with the azides using Click chemistry. A stock solution of **L5** in *N*,*N*-dimethylformamide (DMF) was introduced to plastic reaction vessels, followed by the addition of two equivalents of various azides. Then a catalytic (20 mol%) amount of tetrakis(acetonitrile)copper(I) hexafluorophosphate was added as a solution in DMF. After standing at room temperature for two days, representative reactions from ten vessels were monitored by liquid chromatography–mass spectrometry (LC–MS), which indicated that the reactions furnished products in moderate-to-high conversion with >70% purity. This was consistent with published results from both others and our own group using Click reaction for library assembly.[7g,h,13] To avoid possible false positive hits caused by copper and other impurities, each reaction mixture was diluted with water, and the precipitate formed was filtered

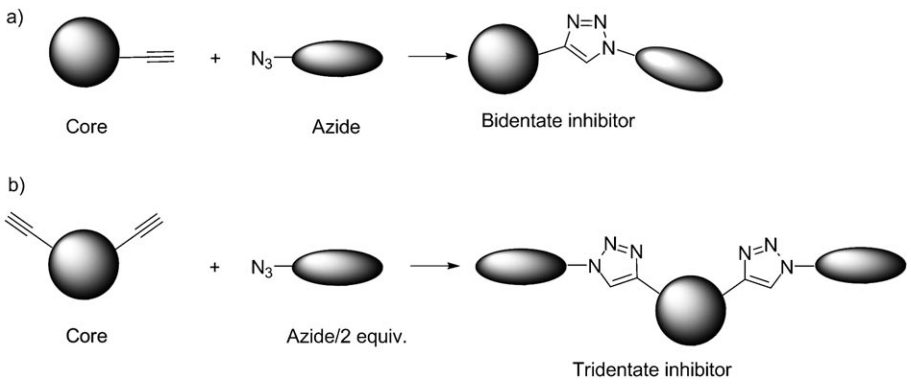

Scheme 1. From a conventional to a double Click reaction: a) conventional Click reaction; b) double Click reaction.

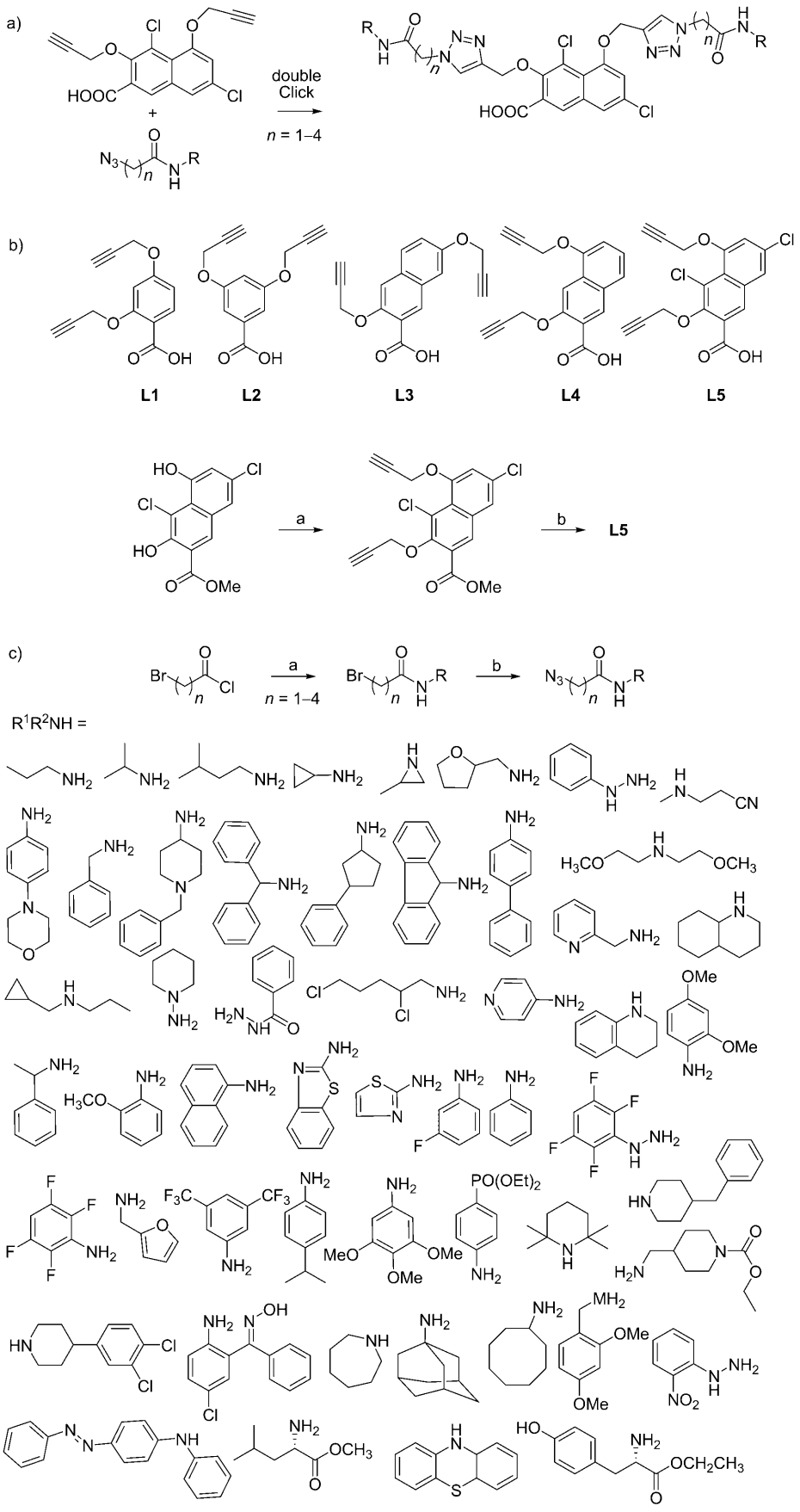

Scheme 2. The Assembly of a compound library by double Click reaction. a) Library generation by double Click reaction. b) The structures and synthesis of cores. *Reagents and conditions*: a) Propargyl bromide (3 equiv), K_2CO_3 (3 equiv), acetone, reflux, overnight; b) 10% NaOH, MeOH, RT, overnight. c) The structures and synthesis of azides. *Reagents and conditions*: a) RNH_2; b) NaN_3, 50–90% yield (two steps).

and washed with water. The solid we collected was dissolved in DMSO to make a 20 mM stock solution, which was ready for the screening step.

To identify mPTPB inhibitors, the ability of the library to inhibit the mPTPB-catalyzed hydrolysis of *p*-nitrophenyl phosphate (*p*NPP) was assessed at pH 7 and 25 °C. Among the 212 members in the library, two compounds displayed excellent inhibitory activity at ~10 μM concentration. Resynthesis of the hits confirmed that they were genuine inhibitors of mPTPB with IC_{50} values in the nanomolar range. Compound **L5B47** (Figure 1a) appeared to be the most potent inhibitor of mPTPB, with an IC_{50} value of 160±10 nM and was selected for further characterization. It should be noted that the IC_{50} value for **L5B47** is 469-fold lower than that of the parent core **L5**, indicating that the linker and amine diversity element contribute significantly to mPTPB binding. The second hit compound, **L5D47** had an IC_{50} value of 270 nM for mPTPB (see the Supporting Information).

Kinetic analysis revealed that **L5B47** is a reversible and noncompetitive inhibitor of mPTPB with a K_i value of 162±10 nM (Figure 1b). To determine the specificity of **L5B47**, its inhibitory activities against mPTPA and a panel of mammalian PTPs, including cytosolic PTPs, PTP1B, TC-PTP, SHP2, Lyp and FAP1, the receptor-like PTPs, CD45, LAR, and PTPα, the dual specificity

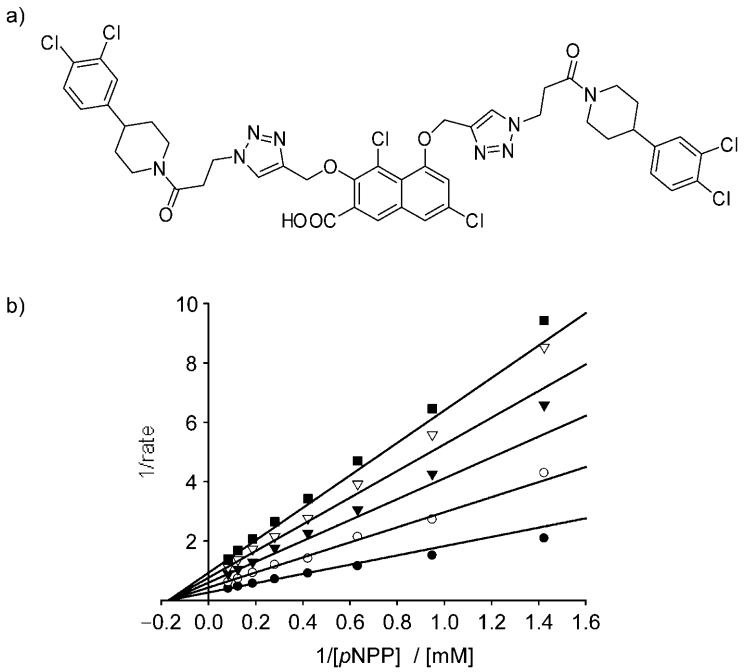

Figure 1. a) Structure of **L5B47**; b) Lineweaver–Burk plot for **L5B47**-mediated mPTPB inhibition. **L5B47** concentrations were 0 (●), 0.1 (○), 0.2 (▼), 0.3 (▽), and 0.4 (■) μM.

phosphatases, VHR, VHX, Cdc14, and the low molecular weight PTP, were measured. As shown in Figure 2, **L5B47** is highly selective for mPTPB, exhibiting a 50-fold preference for mPTPB over mPTPA and greater than 25-fold preference for mPTPB over all mammalian PTPs examined. These results show that **L5B47** is among the most potent and specific mPTPB inhibitors reported to date. Its easy synthesis (three linear chemical steps) offers numerous benefits for further developments. We also prepared compound **L5′B47**, a single Click reaction product from the same core and the same azide. The IC_{50} value of **L5′B47** against mPTPB (3.2 μM) is 20-fold higher (i.e., 20-fold less potent affinity) than **L5B47**. Moreover, **L5′B47** exhibits no selectivity against the same panel of PTPs. Therefore, the double Click chemistry strategy is indeed superior to the conventional single Click reaction in producing more potent and selective mPTPB inhibitors.

Given its exceptional potency and selectivity, we performed a modeling study in order to aid the understanding of potential interactions between **L5B47** and mPTPB. Docking of the inhibitor to mPTPB was carried out using the AutoDock 4.01 software package[14] and the coordinates of mPTPB–OMTS complex (PDB: 2OZ5).[7f] As shown in Figure 3, **L5B47** is predicted to bind near the entrance of the active site, with the carbon atom of the carboxyl group on the naphthalene being 16.3 Å from the sulfur atom on the catalytic Cys160. This predicted binding pose supports the theory that this inhibitor does not compete with the artificial substrate *p*NPP at the catalytic site, which explains the aforementioned kinetic observation that **L5B47** is a reversible and noncompetitive inhibitor of mPTPB. The carboxylate group could

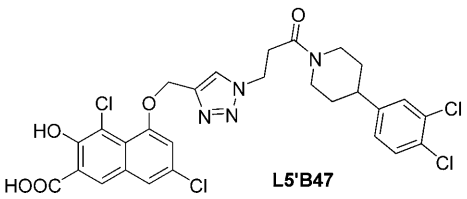

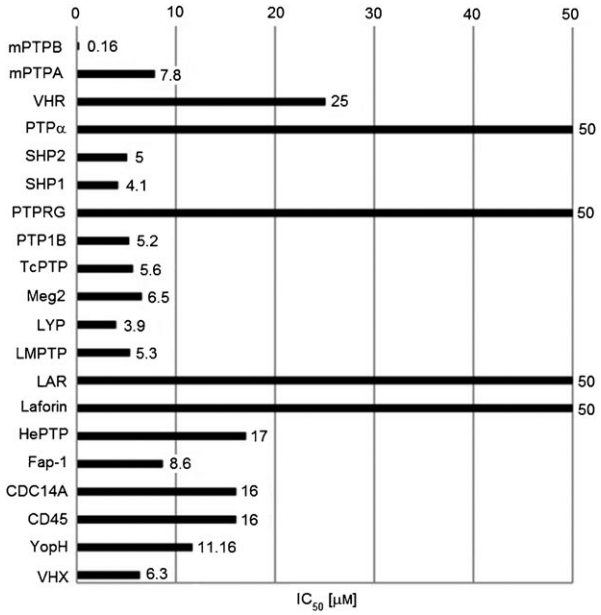

Figure 2. IC_{50} values (μM) of **L5B47** against a panel of PTPs.

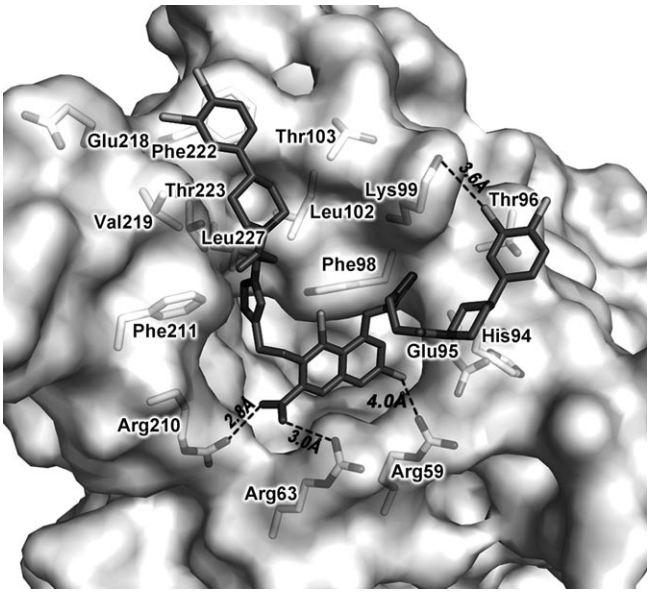

Figure 3. A model for potential interactions between mPTPB and **L5B47**.

potentially form two hydrogen bonds with the η-nitrogen of Arg 210 and Arg 63, which might be important for anchoring the naphthalene core right at the entrance of the active site. The piperidine and chlorine benzene from the carboxylate proximal branch in **L5B47** might sit in a hydrophobic pocket interacting with Phe 98, Leu 102, Phe 222, Val 219 and Leu 227. The carboxylate distal branch of **L5B47** extends to complement a neighboring groove on the surface of mPTPB; it is predicted to make Van der Waals contacts with the surrounded residues, including Arg 59, His 94, Glu 95, Thr 96 and Phe 98. Additionally, weak polar interactions might also exist between the chlorines on the naphthalene and benzene rings and the side chains of Arg 59 and Lys 91, respectively. Interestingly, the majority of the residues implicated in the model of **L5B47** binding appear to be unique to mPTPB, which is consistent with the observed selectivity of **L5B47** for mPTPB.

Conclusions

We demonstrate in this study that, by adding two fragments into the core structure simultaneously, the double Click strategy is superior to the conventional Click reaction for acquisition of more potent and selective enzyme inhibitors. We have identified **L5B47** as the most potent and selective, yet easily accessible, mPTPB inhibitor through this double Click chemistry strategy. **L5B47** inhibits mPTPB in a noncompetitive manner with a K_i value of 160 nM and a selectivity of more than 25-fold for mPTPB over 19 other PTPs. Molecular docking analysis suggests a unique binding mode, in which **L5B47** binds at the entrance of the active site with the two branches occupying hydrophobic grooves on either side. We anticipate the double Click chemistry approach to have broad applicability in the development of multidentate inhibitors directed against other enzymes, in addition to the protein phosphatases.

Experimental Section

Materials: *p*-Nitrophenyl phosphate (*p*NPP) was purchased from Fluke. Dithiothreitol (DTT) was provided by Fisher (Fair Lawn, NJ, USA). For organic synthesis, reagents were used as purchased from Aldrich, Acros, Alfa Aesar or TCI, except where noted. ^{1}H and ^{13}C NMR spectra were obtained on a Bruker Avance II 500 MHz NMR spectrometer with trimethylsilane (TMS) or residual solvent as an internal standard. All column chromatography was performed using 230–400 mesh silica gel (SiO_2; Dynamic Adsorbents) with the solvent system indicated unless otherwise noted. Thin-layer chromatography (TLC) analysis was performed using 254 nm glass-backed plates and visualized using UV light (254 nm). High-pressure liquid chromatography (HPLC) purification was carried out on a Waters Delta 600 equipped with a Sunfire Prep C18 OBD column (30 mm × 150 mm, 5 μm) with MeOH/H_2O (both containing 0.1% TFA) as the mobile phase (gradient: 50–100% MeOH; flow rate: 10 mL min^{-1}). The purity of all final tested compounds was established to be >98% by reverse-phase HPLC on a Waters Breeze HPLC system with a SunFire C18 analytical column (4.6 mm × 150 mm, 5 μm) using CH_3CN/H_2O (both containing 0.1% TFA) as the mobile phase (gradient: 30–100% CH_3CN; flow rate: 1.5 mL min^{-1}), with UV monitoring at a fixed wavelength of 254 nm. Mass spectra were obtained using an Agilent Technologies 6130 quadrupole LC–MS.

Representative procedure for the synthesis of cores (L1–5): A solution of methyl 4,7-dichloro-3,5-dihydroxy-2-naphthoate (0.287 g, 1 mmol) in acetone (3 mL) was treated with K_2CO_3 (0.42 g, 3 mmol) and propargyl bromide (0.32 mL, 80% *w*/*w* in toluene, 3 mmol), and the mixture was heated at reflux overnight. The reaction was concentrated in vacuo, diluted with H_2O (10 mL) and extracted with EtOAc (3×10 mL). The combined organic layer was dried (Na_2SO_4), filtered and concentrated in vacuo. Purification by column chromatography (EtOAc/hexane; 1:5) gave the intermediate (methyl 4,7-dichloro-3,5-bis(prop-2-yn-1-yloxy)-2-naphthoate) as a white solid (0.362 g, 99% yield). Subsequently, the intermediate was dissolved in MeOH (2 mL), and the solution was treated with 20% aq NaOH (2 mL). The mixture was stirred at RT overnight. This reaction was acidified with aq HCl (2 M, 10 mL), and extracted with EtOAc (3×10 mL). The combined organic layer was dried (Na_2SO_4), filtered and concentrated in vacuo. HPLC purification gave **L5** as a white solid (0.312 g, 90%; >95% purity): ^{1}H NMR (500 MHz, $CDCl_3$): δ = 8.39 (s, 1H), 7.80 (s, 1H), 7.74 (s, 1H), 5.07 (d, J = 2.3 Hz, 2H), 4.94 (d, J = 2.4 Hz, 2H), 3.69 (t, J = 2.3 Hz, 1H), 3.66 ppm (t, J = 2.4 Hz, 1H); ^{13}C NMR (500 MHz, $CDCl_3$): δ = 166.5, 154.2, 147.8, 131.7, 127.7, 125.7, 125.6, 125.0, 124.1, 104.3, 99.5, 79.8, 79.3, 78.7, 78.3, 61.4, 56.4 ppm; MS (ESI+): *m*/*z* (%): 349.0 (100%) $[M+H]^+$.

L1: white solid (0.217 g, 94% yield; >95% purity): ^{1}H NMR (500 MHz, $CDCl_3$): δ = 12.40 (s, 1H), 7.74 (d, , J = 8.7 Hz, 1H), 7.67 (d, J = 2.2 Hz, 1H), 6.69 (m, 1H), 4.87 (s, 4H), 3.59 (t, J = 2.3 Hz, 1H), 3.56 ppm (t, J = 2.3 Hz, 1H); ^{13}C NMR (500 MHz, $CDCl_3$): δ = 166.4, 161.2, 158.2, 133.2, 114.3, 106.5, 101.8, 78.9, 78.7, 78.7, 56.3, 55.9 ppm; MS (ESI+): *m*/*z* (%): 231.1 (100%) $[M+H]^+$.

L2: white solid (0.220 g, 95% yield; >95% purity): ^{1}H NMR (500 MHz, $CDCl_3$): δ = 13.1 (s, 1H), 7.19 (d, J = 2.3 Hz, 2H), 6.86 (t, J = 2.3 Hz, 1H), 4.85 (d, J = 2.3 Hz, 4H), 3.69 ppm (t, J = 2.3 Hz, 2H); ^{13}C NMR (500 MHz, $CDCl_3$): δ = 166.9, 158.3, 133.0, 108.4, 107.0, 78.9, 78.6, 55.8 ppm; MS (ESI+): *m*/*z* (%): 231.1 (100%) $[M+H]^+$.

L3: white solid (0.256 g, 91% yield; >95% purity): ^{1}H NMR (500 MHz, $CDCl_3$): δ = 12.97 (s, 1H), 8.16 (s, 1H), 7.80 (d, J = 9.1 Hz, 1H), 7.47 (m, 2H), 7.27 (dd, J = 2.5, 9.0 Hz, 1H), 4.94 (d, J = 2.3 Hz, 2H), 4.90 (d, J = 2.3 Hz, 2H), 3.59 ppm (m, 2H); ^{13}C NMR (500 MHz, $CDCl_3$): δ = 167.4, 154.3, 151.4, 130.6, 129.9, 128.4, 128.3, 124.2, 120.7, 109.0, 108.5, 79.2, 78.5, 78.4, 56.2, 55.6 ppm; MS (ESI+): *m*/*z* (%): 281.1 (100%) $[M+H]^+$.

L4: white solid (0.253 g, 90% yield; >95% purity): ^{1}H NMR (500 MHz, $CDCl_3$): δ = 13.1 (s, 1H), 8.26 (s, 1H), 7.69 (s, 1H), 7.58 (d, J = 8.2 Hz, 1H), 7.36 (t, J = 7.8 Hz, 1H), 7.13 (d, J = 7.7 Hz, 1H), 5.05 (s, 2H), 5.00 (s, 2H), 3.62 ppm (m, 2H); ^{13}C NMR (500 MHz, $CDCl_3$): δ = 167.3, 152.6, 151.5, 131.0, 128.6, 126.7, 124.7, 124.3, 121.3, 108.2, 102.7, 79.2, 79.0, 78.8, 78.7, 56.2, 56.1 ppm; MS (ESI+): *m*/*z* (%): 281.1 (100%) $[M+H]^+$.

Azide synthesis: All of the azides were synthesized previously.[7h,13]

Library synthesis via double Click chemistry: **L5** (0.05 mmol, 0.5 mL of 100 mM stock solution in DMF), azide (0.10 mmol, 2 equiv), and tetrakis(acetonitrile)copper(I) hexafluorophosphate (0.01 mmol, 0.1 mL of 100 mmol stock solution in DMF, 20 mol%) were added to a 2 mL plastic vessel. The vessel was allowed to stand at RT for 2 days. The mixture was then poured into H_2O (6 mL), and the precipitate formed was collected by filtration and washed with H_2O (2×6 mL). The solid collected was dissolved in

DMSO (2 mL) to give a stock solution at 20 mM (assuming the product is obtained at 80% yield).

L5B47: white solid (0.042 g, 85%, >95% purity after HPLC): ^{1}H NMR (500 MHz, $CDCl_3$): δ = 8.35 (s, 1H), 8.31 (s, 1H), 8.28 (s, 1H), 7.72 (m, 2H), 7.34 (m, 2H), 7.09 (m, 2H), 6.88 (m, 2H), 5.33 (s, 2H), 5.23 (s, 2H), 4.61 (m, 4H), 3.50 (m, 8H), 3.13 (m, 8H), 3.06 (t, J = 6.8 Hz, 2H), 2.98 ppm (t, J = 6.8 Hz, 2H); ^{13}C NMR (500 MHz, $CDCl_3$): δ = 206.5, 167.9, 167.8, 166.6, 155.0, 150.3, 150.3, 148.1, 142.0, 141.9, 131.8, 131.5, 131.5, 130.4, 130.4, 127.3, 127.2, 125.7, 125.5, 125.3, 125.2, 124.8, 124.0, 119.9, 116.5, 116.4, 115.4, 103.8, 99.5, 66.4, 62.1, 47.6, 47.3, 45.8, 44.1, 44.1, 40.6, 40.4, 32.7, 32.6, 30.7 ppm; MS (ESI+): m/z (%): 1001.1 (10%) $[M+H]^+$; HRMS calcd. for $C_{45}H_{43}Cl_6N_8O_6$ ($M+H^+$): m/z 1001.1431; found 1001.1556.

L5′B47: white solid (0.028 g, 87%, >95% purity after HPLC): ^{1}H NMR (500 MHz, $CDCl_3$): δ = 8.63 (s, 1H), 8.31 (s, 1H), 7.65 (s, 1H), 7.42 (m, 1H), 7.31 (d, J = 9.0 Hz, 1H), 7.08 (d, J = 2.4 Hz, 1H), 6.88 (dd, J = 8.9, 2.2 Hz, 1H), 5.15 (s, 2H), 4.63 (t, J = 6.4 Hz, 2H), 3.56 (m, 4H), 3.14 (m, 4H), 3.02 ppm (t, J = 6.4 Hz, 2H); ^{13}C NMR (500 MHz, $CDCl_3$): δ = 167.9, 157.8, 150.3, 147.6, 141.9, 133.5, 131.4, 130.3, 128.6, 127.9, 125.5, 125.2, 124.6, 123.3, 119.9, 116.4, 115.4, 114.5, 106.7, 99.5, 66.2, 47.6, 47.2, 45.8, 44.2, 40.6, 40.4, 32.7 ppm; MS (ESI+): m/z (%): 637.1 (10%) $[M+H]^+$.

Inhibition study: Expression and purification of recombinant mPTPB, and kinetic characterization of mPTPB inhibitors were performed as described previously.[7h]

Docking analysis: The AutoDock 4.0 software package[14] was used to build the binding model of **L23B47** with mPTPB. The three-dimensional structure of **L23B47** was modeled and energy minimized in Chem3D program (ChemBio3D Ultra 12.0), and the coordinates of mPTPB were taken from an mPTPB–OMTS complex structure (PDB: 2OZ5).[7f] Both ligand and receptor were introduced into AutoDockTools 1.4.6[15] for a series of preprocessing, such as merging nonpolar hydrogen atoms, adding Gasteiger charges, setting rotatable bonds for the ligand, adding solvation parameters for the receptor, and so on. The docking space was visually set around the active site, the energy-grid size was set to 66×60×80 points with 0.375 Å spacing on each axis, then the energy-grid maps for each atom type found in **L23B47** (i.e., A, C, N, NA, OA and Cl), as well as the electrostatic forces and desolvation maps were calculated using the auxiliary program of AutoGrid 4. Based on all of these prepared files, the automatic molecular docking work was carried out using the AutoDock 4 program, the Lamarckian genetic algorithm with local search (LGALS) was selected for ligand conformational searching, the optimal binding conformation was determined by the LGALS algorithm with the following important parameters during each docking run: energy evaluations of 2500000, population size of 100, mutation rate of 0.02, crossover rate of 0.8, Solis and Wets local search iterations of 300 with a probability of 0.06. Finally, 256 separate docking runs were performed, and the resulting 256 binding conformations were classified into different clusters and ranked according to the calculated binding free energy. These cluster and energy information, together with visual inspection in AutoDockTools 1.4.6, generate the most possible binding mode.

Acknowledgements

This work was supported in part by the National Institutes of Health (NIH; USA) (grants: CA69202 and CA126937).

Keywords: Click chemistry · drug design · protein tyrosine phosphatases · inhibitors · tuberculosis

[1] a) N. K. Tonks, B. G. Neel, *Curr. Opin. Cell Biol.* **2001**, *13*, 182–195; b) A. Alonso, J. Sasin, N. Bottini, I. Friedberg, I. Friedberg, A. Osterman, A. Godzik, T. Hunter, J. Dixon, T. Mustelin, *Cell* **2004**, *117*, 699–711; c) N. K. Tonks, *Nat. Rev. Mol. Cell Biol.* **2006**, *7*, 833–846.
[2] Z.-Y. Zhang, *Curr. Opin. Chem. Biol.* **2001**, *5*, 416–423.
[3] A. Koul, T. Herget, B. Klebl, A. Ullrich, *Nat. Rev. Microbiol.* **2004**, *2*, 189–202.
[4] a) A. Koul, A. Choidas, M. Treder, A. K. Tyagi, K. Drlica, Y. Singh, A. Ullrich, *J. Bacteriol.* **2000**, *182*, 5425–5432; b) R. Singh, V. Rao, H. Shakila, R. Gupta, A. Khera, N. Dhar, A. Singh, A. Koul, Y. Singh, M. Naseema, P. R. Narayanan, C. N. Paramasivan, V. D. Ramanathan, A. K. Tyagi, *Mol. Microbiol.* **2003**, *50*, 751–762.
[5] a) D. Butler, *Nature* **2000**, *406*, 670–672; b) D. Maher, M. Raviglione, *Clin. Chest Med.* **2005**, *26*, 167–182.
[6] a) Y. Zhang, *Annu. Rev. Pharmacol. Toxicol.* **2005**, *45*, 529–564; b) A. E. Clatworthy, E. Pierson, D. T. Hung, *Nat. Chem. Biol.* **2007**, *3*, 541–548; c) Z. Ma, C. Lienhardt, H. McIlleron, A. Nunn, X. Wang, *Lancet* **2010**, *375*, 2100–2109.
[7] a) A. Noren-Muller, I. Reis-Correa, Jr., H. Prinz, C. Rosenbaum, K. Saxena, H. Schwalbe, D. Vestweber, G. Cagna, S. Schunk, O. Schwarz, H. Schiewe, H. Waldmann, *Proc. Natl. Acad. Sci. USA* **2006**, *103*, 10606–10611; b) I. R. Corrêa, Jr., A. Noren-Muller, H.-D. Ambrosi, S. Jakupovic, K. Saxena, H. Schwalbe, M. Kaiser, H. Waldmann, *Chem. Asian J.* **2007**, *2*, 1109–1126; c) A. Nören-Müller, W. Wilk, K. Saxena, H. Schwalbe, M. Kaiser, H. Waldmann, *Angew. Chem.* **2008**, *120*, 6061–6066; *Angew. Chem. Int. Ed.* **2008**, *47*, 5973–5977; d) T. Weide, L. Arve, H. Prinz, H. Waldmann, H. Kessler, *Bioorg. Med. Chem. Lett.* **2006**, *16*, 59–63; e) M. B. Soellner, K. A. Rawls, C. Grundner, T. Alber, J. A. Ellman, *J. Am. Chem. Soc.* **2007**, *129*, 9613–9615; f) C. Grundner, D. Perrin, R. H. V. Huijsduijnen, D. Swinnen, J. Gonzalez, C. L. Gee, T. N. Wells, T. Alber, *Structure* **2007**, *15*, 499–509; g) L. P. Tan, H. Wu, P.-Y. Yang, K. A. Kalesh, X. Zhang, M. Hu, R. Srinivasan, S. Q. Yao, *Org. Lett.* **2009**, *11*, 5102–5105; h) B. Zhou, Y. He, X. Zhang, J. Xu, Y. Luo, Y. Wang, S. G. Franzblau, Z. Yang, R. Chan, Y. Liu, J. Zheng, Z.-Y. Zhang, *Proc. Natl. Acad. Sci. USA* **2010**, *107*, 4573–4578.
[8] Z.-Y. Zhang, *Annu. Rev. Pharmacol. Toxicol.* **2002**, *42*, 209–234.
[9] Y. A. Puius, Y. Zhao, M. Sullivan, D. S. Lawrence, S. C. Almo, Z.-Y. Zhang, *Proc. Natl. Acad. Sci. USA* **1997**, *94*, 13420–13425.
[10] H. C. Kolb, M. G. Finn, K. B. Sharpless, *Angew. Chem.* **2001**, *113*, 2056–2075; *Angew. Chem. Int. Ed.* **2001**, *40*, 2004–2021.
[11] a) H. C. Kolb, K. B. Sharpless, *Drug Discovery Today* **2003**, *8*, 1128–1137; b) M. Meldal, C. W. Tornoe, *Chem. Rev.* **2008**, *108*, 2952–03015; c) J. C. Jewett, C. R. Bertozzi, *Chem. Soc. Rev.* **2010**, *39*, 1272–1279.
[12] a) K. Shen, Y.-F. Keng, L. Wu, X.-L. Guo, D. S. Lawrence, Z.-Y. Zhang, *J. Biol. Chem.* **2001**, *276*, 47311–47319; b) S. Zhang, L. Chen, Y. Luo, A. Gunawan, D. S. Lawrence, Z.-Y. Zhang, *J. Am. Chem. Soc.* **2009**, *131*, 13072–13079.
[13] a) X. Yu, J.-P. Sun, Y. He, X.-L. Guo, S. Liu, B. Zhou, A. Hudmon, Z.-Y. Zhang, *Proc. Natl. Acad. Sci. USA* **2007**, *104*, 19767–19772; b) X. Zhang, Y. He, S. Liu, Z. Yu, Z.-X. Jiang, Z. Yang, Y. Dong, S. C. Nabinger, L. Wu, A. M. Gunawan, L. Wang, R. J. Chan, Z.-Y. Zhang, *J. Med. Chem.* **2010**, *53*, 2482–2493.
[14] a) G. M. Morris, D. S. Goodsell, R. S. Halliday, R. Huey, W. E. Hart, R. K. Belew, A. J. Olson, *J. Comput. Chem.* **1998**, *19*, 1639–1662; b) R. Huey, G. M. Morris, A. J. Olson, D. S. Goodsell, *J. Comput. Chem.* **2007**, *28*, 1145–1152.
[15] M. F. Sanner, *J. Mol. Graphics Model.* **1999**, *17*, 57–61.

Received: August 14, 2010
Published online on October 18, 2010

